Author's Accepted Manuscript

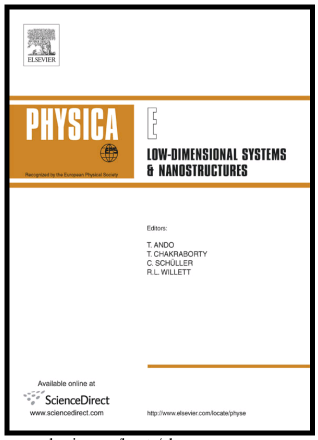

www.elsevier.com/locate/physe

Aligned magnetic field effects on water based metallic nanoparticles over a stretching sheet with PST and thermal radiation effects

Irfan Rashid, Rizwan Ul Haq, Qasem M. Al-Mdallal

PII: S1386-9477(16)30434-9
DOI: http://dx.doi.org/10.1016/j.physe.2017.01.029
Reference: PHYSE12720

To appear in: *Physica E: Low-dimensional Systems and Nanostructures*

Received date: 18 May 2016
Revised date: 21 December 2016
Accepted date: 4 January 2017

Cite this article as: Irfan Rashid, Rizwan Ul Haq and Qasem M. Al-Mdallal Aligned magnetic field effects on water based metallic nanoparticles over . stretching sheet with PST and thermal radiation effects, *Physica E: Low dimensional Systems and Nanostructures* http://dx.doi.org/10.1016/j.physe.2017.01.029

Aligned magnetic field effects on water based metallic nanoparticles over a stretching sheet with PST and thermal radiation effects

Irfan Rashid[1], Rizwan Ul Haq[2,*], Qasem M. Al-Mdallal[3]
[1]Department of mathematics, Capital university of Science and Technology, Islamabad 44000, Pakistan
[2]Department of Electrical Engineering, Bahria University, Islamabad 44000, Pakistan
[3]Department of Mathematical Sciences, UAE University, Al Ain, P.O. Box 15551, United Arab Emirates

ideal_riz@hotmail.com

r.haq.qau@gmail.com

[*]Corresponding author.

Abstract

This study deals the simultaneous effects of inclined magnetic field and prescribed surface temperature (PST) on boundary layer flow of nanofluid over a stretching sheet. In order to make this mechanism more feasible, we have further considered the velocity slip and thermal radiation effects. Moreover, this perusal is made to consider the two kinds of nanofluid namely: Cu-water and Al_2O_3-water. Inclined magnetic field is utilized to accompanying an aligned angle that varies from 0 to $\pi/2$. The exact solutions are acquired from the transformed non-dimensional momentum and energy equations in the form of confluent hypergeometric function. Lorentz forces and aligned magnetic field depicts the significant effects on nanofluid. We found that, due to the increase in the aligned angle provides the enhancement in local skin friction coefficient and a reduction in the local Nusselt number. The combined impacts of inclined magnetic field with other emerging parameters such as velocity slip, thermal radiation and nanoparticles volume fraction on velocity, temperature, local Nusselt number and skin friction coefficient are examined. Flow behavior of nanofluid is also determined via stream lines pattern.

Graphical Abstract:

Analysis is reported for two different homogenous mixtures namely: Cu-Water and Al_2O_3-Water in the presence of thermal radiation. These vital results are describing the flow behavior via stream lines.

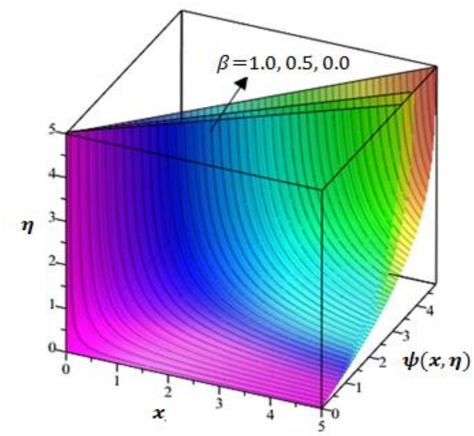

Keywords: Aligned MHD, PST, thermal radiation, nanofluid, heat transfer.

1. Introduction

Magneto-hydrodynamics (MHD) is the investigation of the fluid mechanics connected with electrically conducting fluid along with electro-magnetic physical proceeding that possesses significant industrial achievements. MHD has numerous applications based on its wide use at industrial level. For instance few particular applications are MHD power generators, cooling of nuclear reactors, bearings, Micro MHD pumps and boundary layer influence are impacted by the association into a magnetic field and electrically leading fluid. Hydromantic boundary layers are significantly affected by the magnetic field and electrically conducting fluid. Hydromantic boundary layer watched in a few technical system utilizing fluid metallic and plasma flow like transversal of magnetic field. For instance, the control of flow could be acknowledged through the Lorentz forces. Nowadays, several research articles deal with the boundary layer flow problem by stretching surface in traverse flow under the impact of magnetic field [1-8]. The study of fluid over a stretching sheet is an imperative issue in numerous applications in industrial field such as polymer sheets and fibers production by continuous expulsion of the polymer from a pass on to a windup roller, which is situated at a finite distance away. The number of researchers has discussed the boundary layer issues past a stretching surface into sheet's vicinity and horizontal magnetic extent [9-15].

The increments in viable thermal conductibility have critical impact on enhancing the heat transport conducts of fluids. All through several manufacturing equipment, heat should be conflated, evacuated, as a choice actuated starting with individual procedure flow then onto the next and it has turned into a noteworthy undertaking as industrial requirement. These procedures give an origin to energy recuperation and treat fluid heating as well as refrigerating. The improvement concerning warming/refrigerating within a mechanical procedure might make a preserving into vitality, lessen action time, increase heating appraising and protract the working apparatus existence. The advancement of superior thermal conductivity of liquid for heat transfer improvement has become followed presently. In this manner the appearance of elevated heat flow forms claims critical interest in order to advancements toward improve heat exchange. Researchers have attempted to enhance the characteristically poor thermal conductibility of those conventional heat transfer liquids using the macroscopic effective medium theory (EMT) introduced by Maxwell [16] (1873) for viable properties of mixture. Modern nanotechnology committed the chance to acquire nanometer-sized particles which are very unique in relation to the nurture material in mechanical, electrical, thermal, and optical attributes to improve the heat transfer efficiency compared to the traditional.

The expression "Nanofluids" is utilized for the liquids acquiring of nano-sized metallic/non-metallic particles. Nanofluids are engineered toward suspending nanoparticles having normal volumes underneath 100nm within host fluid for instance, 1, 2-Ethanediol $(CH_2OH)_2$, water and oil. Nanofluids ordinarily utilize metal or metal oxide nanoparticles, for example, copper and alumina. The fundamental thought of utilizing nanoparticles is to improve the thermal attributes of a host fluid. Accomplishment of nanofluids with enhanced thermal uniqueness can be imperative in stipulations of more equipped cooling frameworks, weighty in higher productivity and vitality savings. A few forthcoming applications for nanofluids are heat exchangers, radiators for motors, prepare cooling frameworks, small scale equipment etc.

In the beginning, Choi [17] had started work on incorporating the nanoparticles within the base fluid in 1995. Adjacent to the idea of nanofluid, it was found that heat transfer feasibly magnificent yet at the rate of exceptionally cost pumping power. Choi presumed such a domination connected with heat conductivity is vastly improved of nanofluid compared with exceptionally fetched extracting power for warmth transplant effectiveness. In this manner, integration of nanoparticles inside of the base fluid are not just useful for high thermal framework yet by one means or another it is less expensive monetarily. Nanoparticles are produced using distinctive materials, for example: carbide ceramics (Sic, Tic), metal nitrides (AlN, SiN), oxide ceramics (Al_2O_3, CuO), metals (Cu, Ag, Au), carbons in respective (e.g. diamond, carbon nano tubes, graphite, fullerene) and functionalized nanoparticles [18-22]. Some preparatory exploratory results [23] demonstrated such as increment into warm conductivity of roughly 60% as it may be gotten for the nanofluid comprising of H_2O and 5% of CuO nanoparticles. Masuda et al. [24] have demonstrated that the characteristic boast of nanofluids is thermal conductivity enhancement phenomenon. Recently Buongiorno [25] considered successfully seven slip mechanism recognize inertia, Brownian motion, thermophoresis, Magnus effect, thermos-diffusion, fluid drainage and gravitation settling. He attained an accomplished overview of convective transport in nanofluids. Very recent studies explore that enhancement in the heat transfer in the presence of nanoparticles can play a vital role in various physical geometries [26-40].

Based upon above literature survey, main motivation of the present study is to discuss the nanofluid ($Al_2O_3 -$ water, $Cu -$water) flow over a stretching sheet via inclined Lorentz forces within the boundary layer region which passed through a stretching sheet. Further, we have analyzed the velocity slip and thermal radiation effects for prescribed surface temperature. For the solution of governing PDEs use the similarity transformation to convert the governing partial differential equations into ordinary differential equations. Exact solution of the governing ODEs are obtain in the form of Kummer's function to discuss the nature of flow and heat transfer, velocity and temperature profile are plotted against the emerging parameters. Results are verified with the existing literature.

2. Mathematical formulation

Consider two dimensional, steady, incompressible flow of nanofluid over a stretching sheet with slip effects at the surface. In this context we have considered water as a base fluid and two different kind of metallic nano particles are taken into the account namely: Copper (Cu) and alumina (Al_2O_3). Inclined magnetic field is applied along *y*-axis of strength B_0 with an acute angle γ that is normal to the surface and *x*-axis taken parallel the sheet. That is to suppose influenced magnetic field which is negated in correspondence with enforced magnetic range. The applied magnetic field occurs normal to the surface with transverse magnetic field at $\gamma = \frac{\pi}{2}$ i.e. $sin\left(\frac{\pi}{2}\right) = 1$. The basic governing equations for the problem are:

$$\frac{\partial u}{\partial x} + \frac{\partial u}{\partial y} = 0, \tag{1}$$

$$u\frac{\partial u}{\partial x} + v\frac{\partial u}{\partial y} = \frac{\mu_{nf}}{\rho_{nf}}\frac{\partial^2 u}{\partial y^2} - \frac{\sigma_{nf}B_0^2}{\rho_{nf}}\, u\, sin^2\,\gamma, \tag{2}$$

where u, v are the velocity components of the nanofluid in the directions of x and y-axis respectively, μ_{nf} and ρ_{nf} is the dynamic viscosity and density regarding nanofluid respectively, α_{nf} is the thermal diffusivity, $(\rho C_p)_{nf}$ is the heat capacity of nanofluid, v_{nf} is the kinematic viscosity for the nanofluid that is defined by Tiwari Das [27]:

$$\left.\begin{array}{c} \mu_{nf} = \frac{\mu_f}{(1-\phi)^{2.5}},\ \alpha_{nf} = \frac{k_{nf}}{(\rho C_p)_{nf}}\ , \\ (\rho C_p)_{nf} = (1-\phi)(\rho C_p)_f + \phi(\rho C_p)_s\ , \\ v_{nf} = \frac{\mu_{nf}}{\rho_{nf}}\ , \rho_{nf} = (1-\phi)\rho_f + \phi(\rho)_s\ , \\ \frac{k_{nf}}{k_f} = \frac{(k_s+2k_f)-2\phi(k_f-k_s)}{(k_s+2k_f)+\phi(k_f-k_s)}. \end{array}\right\} \tag{3}$$

The nanoparticle volume fraction parameter is represented by ϕ. In the above expressions subscript f is used for base fluid and s is used for nanoparticle. The boundary conditions for the above model

$$u = ax + l\frac{\partial u}{\partial y}\ , v = v_w \text{ at } y = 0,$$

$$u \to 0 \text{ as } y \to \infty. \tag{4}$$

For sake of simplifying the analysis, we introduced the following similarity transformation:

$$u = axf'(\eta)\ ,v = -\left(a\vartheta_f\right)^{\frac{1}{2}} f(\eta)\ ,\ \eta = \left(\frac{a}{\vartheta}\right)^{1/2}, \tag{5}$$

where $f(\eta)$ and η are dimensionless variables. Using equation (5) shows that equation (1) is completely satisfied whereas equation (2) becomes:

$$\frac{1}{A_1 A_2} f''' + ff'' - \left(f' + \frac{M_2}{A_2}\sin^2(\gamma)\right) f' = 0, \tag{6}$$

subject to the boundary conditions

$$f(\eta) = 0, f'(\eta) = 1 + \frac{\beta}{A_1} f''(\eta) = 1 + Lf''(\eta), \text{ at } \eta = 0,$$

$$f'(\eta) \rightarrow 0 \text{ as } \eta \rightarrow \infty, \tag{7}$$

where $f = f(\eta)$, $A_1 = (1-\phi)^{2.5}$, $A_2 = \left(1 - \phi + \phi\frac{\rho_s}{\rho_f}\right)$, $L = \beta\ /A_1$. In the above equations $M_2 = \sqrt{\frac{\sigma B_0^2}{\rho a}}$ and $\beta = l(a/\vartheta)^{1/2}$ are the Hartmann number and slip parameter, respectively. The closed form solution of equation (6) using (7) can be found as follows

$$f(\eta) = \frac{\chi - \chi e^{-\alpha\eta}}{\alpha}, \tag{8}$$

where,

$$\chi = \frac{1}{L\alpha + 1},$$

and $\alpha = 1/6L(-72M_2A_1L^2\,cos^2\gamma + 72M_2A_1L^2 + 108A_1L^2A_2$

$$-8 + 12\sqrt{3}(A_1(4M_2^3{A^2}_1L^4\,cos^6\gamma - 12M_2^3{A^2}_1L^4\,cos^4\gamma))$$

$$+8M_2^2A_1L^2\,cos^4\gamma + 12M_2^3A_1^2L^4\,cos^2\gamma - 16M_2^2A_1L^2\,cos^2\gamma$$

$$+4\cos^2\gamma\, M_2 - 4M_2^3A_1^2L^4 + 8M_2^2A_1L^2 - 4M_2 - 36M_2A_1L^2\cos^2\gamma\, A_2$$

$$+36M_2A_1L^2A_2 + 27A_1L^2A_2^2 - 4A_2))^{\frac{1}{2}}L)^{\frac{1}{3}} - \frac{2}{3}(3M_2A_1L^2\cos^2\gamma - 3M_2A_1L^2 - 1)/(L$$

$$(-72M_2A_1L^2\cos^2\gamma + 72M_2A_1L^2 + 108A_1L^2A_2 - 8 + 12\sqrt{3}(A_1(4M_2^3A_1^2L^4\cos^6\gamma$$

$$-12M_2^3A_1^2L^4\cos^4\gamma + 8M_2^2A_1L^2\cos^4\gamma + 12M_2^3A_1^2L^4\cos^2\gamma - 16M_2^2A_1L^2\cos^2\gamma$$

$$+4\cos^2\gamma\, M_2 - 4M_2^3A_1^2L^4 + 8M_2^2A_1L^2 - 4M_2 - 36M_2A_1L^2\cos^2\gamma\, A_2$$

$$+36M_2A_1L^2A_2 + 27A_1L^2A_2^2 - 4A_2))^{1/2}L)^{1/3}) - \frac{1}{3L}. \qquad (9)$$

Transform the velocity components by using equations (8) in (4), one obtains

$$u = \frac{axe^{-\alpha\eta}}{L\alpha + 1},\ v = -\sqrt{a\vartheta}\left(\frac{1 - e^{-\alpha\eta}}{\alpha(L\alpha + 1)}\right). \qquad (10)$$

Local skin friction is defined as

$$C_f = \frac{\tau_w}{\rho u_w^2} = \frac{Re_x^{-1/2}}{A_1} f''(0), \qquad (11)$$

where, $\tau_w = \mu_{nf}\left(\frac{\partial u}{\partial y}\right)_{y=0}$ represents the stress at wall and $Re_x = \frac{xu_w}{\vartheta}$ is the Reynolds number.

3. Heat transfer analysis

In this section we have analyzed the basic thermal boundary layer partial differential equation for incompressible nanofluid, expressed in this way:

$$u\frac{\partial T}{\partial x} + v\frac{\partial T}{\partial y} = \alpha_{nf}\frac{\partial^2 T}{\partial y^2} - \frac{1}{(\rho C_p)_{nf}}\frac{\partial q_r}{\partial y}, \qquad (12)$$

where, k_{nf} is thermal conductivity of the nanofluid, ρ_{nf} is the density of the nanofluid, T is the temperature and $(Cp)_{nf}$ represents the specific heat of nanofluid. Utilizing the Roseland diffusion approximation [28] as radiation, the heat flux is defined as,

$$q_r = -\frac{\sigma^*}{3k_*}\frac{\partial T^4}{\partial y}, \tag{13}$$

where σ^* represents the Stefan's constant and k_* stands for the mass absorption coefficient. Additionally, we suppose that the variance of temperature inside of the nanofluid flow is abundantly small in such a way T^4 can be able expressed in a Taylor series lose to T_∞. Further, ignore the terms which have higher order. As follows

$$T^4 \cong 4T_\infty^3 T - 3T_\infty^3. \tag{14}$$

Applying equation (13) and (14) in (12), one obtains

$$u\frac{\partial T}{\partial x} + v\frac{\partial T}{\partial y} = \alpha_{nf}\frac{\partial^2 T}{\partial y^2} + \frac{1}{3(\rho C_p)_{nf}}\frac{16\sigma^* T_\infty^3}{k_*}\frac{\partial^2 T}{\partial y^2}. \tag{15}$$

Notice that equation (15) is solved by using the inclusive heating procedure for instance prescribed surface temperature (PST). In this situation the boundary conditions should be given by

$$T = T_w = T_\infty + A\left(\frac{x}{l}\right)^2 \text{at } y = 0,$$

$$T \to \infty \text{ as } y \to \infty, \tag{16}$$

where, T_w is the sheet temperature, the temperature of the nanofluid far from the surface is represented by T_∞ and l is characteristics length. One the other hand, the dimensionless temperature profile $\theta(\eta)$ is given by

$$\theta(\eta) = \frac{T - T_\infty}{T_w - T_\infty}. \quad (17)$$

Now, we transform the equation (15) by using Eqs. (5) and (17). We get the dimensionless ODE for temperature that is

$$\omega\theta_{\eta\eta} + Prf\theta_\eta - 2Prf_\eta\theta = 0, \quad (18)$$

where, η subscript shows the derivative with respect to the η, $Pr = \nu_f/\alpha_f$ is the Prandtl number, and $N = k_* K_f/4\sigma^* T_\infty^3$ is the radiation parameter. It should be noted that $A_3 = \frac{(k_s+2k_f)-2\phi(k_f-k_s)}{(k_s+2k_f)+\phi(k_f-k_s)}$, $A_4 = (1 - \phi + \phi\frac{(\rho C_p)_s}{(\rho C_p)_f})$ and $\omega = \frac{A_3}{A_4}(3NA_3 + 4)/3NA_3$.

Accordingly, the boundary condition (16) becomes

$$\theta(\eta) = 1 \quad \text{at} \quad \eta = 0,$$

$$\theta(\eta) \to 0 \text{ at } \eta \to \infty. \quad (19)$$

Using the value of f and f_η from equation (8) in (18), we obtain

$$\omega\theta_{\eta\eta} + Pr\chi(\frac{1-e^{-\alpha\eta}}{\alpha})\theta_\eta - 2Pr\chi(\frac{\alpha e^{-\alpha\eta}}{\alpha})\theta = 0. \quad (20)$$

Here we introduced a new variable $\xi = -\frac{A_4}{A_3}\frac{Pr\chi e^{-\alpha\eta}}{\omega\alpha^2}$ and the equation (20) reduces to

$$\xi\frac{\partial^2\theta}{\partial\xi^2} + (h - \xi)\frac{\partial\theta}{\partial\xi} - g\theta = 0, \quad (21)$$

Where $h = (1 - \frac{Pr\chi}{\omega\alpha^2})$ and $g = -2$.

Subject to the boundary conditions

$$\theta\left(-\frac{Pr\chi e^{-\alpha\eta}}{\omega\alpha^2}\right) = 1,$$

$$\theta(0) = 1, \tag{22}$$

the solution of equation (21) is given by

$$\theta(\xi) = (\xi)^{\frac{a+b}{2}} \frac{M\left(\frac{a+b-4}{2},1+b,\xi\right)}{M\left(\frac{a+b-4}{2},1+b,-b\right)}, \tag{23}$$

where $b = \frac{Pr\chi}{\omega\alpha^2}$, M is the confluent hypergeometric function of the Kummer function and so the temperature solution takes the form

$$\theta(\eta) = e^{-\alpha\left(\frac{a+b}{2}\right)\eta} \; \frac{M\left(\frac{a+b-4}{2},1+b,-\frac{Pr\chi e^{-\alpha\eta}}{\omega\alpha^2}\right)}{M\left(\frac{a+b-4}{2},1+b,-\frac{Pr\chi}{\omega\alpha^2}\right)}\,. \tag{24}$$

Hence the non-dimensional wall temperature is found to be

$$\theta_\eta(0) = -\alpha\left(\frac{a+b}{2}\right) + \left(\frac{M\left(\frac{a+b-2}{2},1+b,\frac{Pr\chi}{\omega\alpha^2}\right) - M\left(\frac{a+b-4}{2},1+b,-\frac{Pr\chi e^{-\alpha\eta}}{\omega\alpha^2}\right)}{M\left(\frac{a+b-4}{2},1+b,-\frac{Pr\chi}{\omega\alpha^2}\right)}\right)\left(\frac{a+b-4}{2}\right)\alpha. \tag{25}$$

Note that, the local Nusselt number is given by

$$Nu = \frac{xq_w}{k_f(T_w - T_\infty)}, \tag{26}$$

where $q_w = -\left(k_{nf} + \frac{16\sigma^* T_\infty^3}{3k_*}\right)\left(\frac{\partial T}{\partial y}\right)_{y=0}$. In the current case, it is determined as

$$Nu_x Re_x^{-(1/2)} = -(A_3 + \frac{4}{3N})\theta'(0). \tag{27}$$

4. Results and discussion

In this section, we analyzed the effects of inclined magnetic field along with the other physical parameters in fluid flow characteristics over a stretching sheet. In **table 1**, thermo-physical properties of water and each nanoparticle are presented in the form density, specific heat and thermal conductivity. Before going to discuss the behavior of effective profiles we have made comparison with the available results in the literature. It is clearly seen that our results are accurate for limiting case in comparison with the Hakeem et al. [1] and Turkyilmazoglu [9] (see **table 2**). We have examined the two important kinds of nanoparticles, namely: copper (Cu) and alumina (Al_2O_3), within the base fluid water. Influence of nanoparticles volume fraction ϕ with the base fluid water are described through velocity and temperature for prescribed surface heat flux (See Fig. 1 and Fig. 4). It can be examined in Fig. 1(a), an increase of nanoparticle volume fraction ϕ decreases the velocity behavior of nanofluid (Cu-water). In case of Al_2O_3-water, it is found that an increase the nanoparticle volume fraction gives the rise in velocity profile Fig. 1(b). In Figs. 4(a) and 4(b), the temperature profile described the behavior of Cu-water and Al_2O_3-water with increasing the nanoparticle volume friction ϕ. Figs. 2, 4, 5 and 7 depict the simultaneous effect of angle and Hartmann number M_2 on the velocity and temperature for each Cu and Al_2O_3nanoparticles. It is found that with the increase of magnetic parameter M_2 and aligned angle of magnetic field cause decreasing effects on velocity profile; however it enhances the temperature distribution. There is no impact of magnetic field at velocity profile for $\gamma = 0°$ and the magnetic field behave transversely encase of $\gamma = \pi/2$ along the flow section. The magnetic induction increases with an increase in aligned angle values along the flow region. Due to the improvement of magnetic induction, there is a force called Lorentz force which produces a resistant within the boundary layer with aligned magnetic field. This figure acknowledging the physical action that velocity profile deceases and temperature profile increases gradually for both Cu-water and Al_2O_3-water.

Table 1: Thermophysical properties of Cu, Al_2O_3 and water [29].

Physical properties	Water/base fluid	Cu	Al_2O_3
ρ (kg/m^3)	997.1	8933	3970
C_p(J/kg K)	4179	385	765
k (W/m K)	0.613	400	40
Pr	6.2		

Table 2: Comparison of PST for $\theta_\eta(0)$ when $\phi = \beta = M_2 = N = 0$.

Mn	Pr	Turkyilmazoglu [9]	Hakeem et al. [1]		Present study
		Exact solution	Analytical	Numerical	Exact solution
0	1	1.33333	1.33333	1.3333333	1.33333
	5	3.31648	3.31648	3.3164824	3.31648
1	1	1.21577	1.21577	1.2157726	1.21577
	5	-	3.20720	3.2072054	3.20720

The importance of the slip parameter L on the nanofluid velocity profile and the temperature profile with prescribed surface temperature are plotted in Figs. 3 and 6 at different nanoparticles volume fraction ϕ. In Fig. 3, it can be determined that velocity profile switch its behavior at $\eta = 2.2$ due to the slip effects in the vicinity of sheet surface. The temperature profile increases in same manners with increasing values of velocity slip parameter for both Cu −water and Al_2O_3 − water (see Fig. 6). The nanofluid velocity and temperature profile behave oppositely with increasing value of slip condition. This behavior of stretching sheet can comprise just partially carried to the fluid. Figs. 8(a) and 8(b) describe the effects of radiation parameter on temperature profile for each Cu −water and Al_2O_3 −water, respectively. It can determine that temperature is decreasing function of radiation parameter N.

Figs. 9(a) and 9(b) depict the magnetic parameter influences herewith the solid volume fraction ϕ and aligned angle on local skin friction coefficient. Here magnetic parameter and local skin friction is taken along the *x*- and *y*-axis respectively. In Fig. 9(a), the local skin friction increases by a gain in the aligned angle and magnetic parameter. Since there is no effect of magnetic parameter with $\gamma = 0°$ on local skin friction, it shows the less magnetic parameter effects on the flow section. In Fig. 9(b), one can see the increasing behavior of local skin friction by increasing the nanoparticles volume fraction ϕ and magnetic parameter M_2. Further, it is noticed that Cu-water nanofluid has higher frication with surface as compared to the Al_2O_3-water.

Figs. 10(a) and 10(b) illustrate the effects of magnetic parameter and the volume fraction ϕ on local Nusselt number. It can be seen that the local Nusselt number increases as the values of nanoparticle volume fraction ϕ increases. In Fig. 10(a), it is found that Cu-water represents the heat transfer rate is faster than Al_2O_3-water. In Fig. 10(b) the local Nusselt number decreases with both velocity slip and magnetic parameter for both Cu-water and Al_2O_3-water. Furthermore, it is observed that Al_2O_3-water has low heat transfer rate compare to the Cu-water. The combined results for aligned angle and magnetic parameter are shown in Fig. 11(a) which shows that these parameters reducing the behavior of local Nusselt number. The local Nusselt number is decreasing function with radiation and magnetic parameters for both Cu-Water and Al_2O_3-water (see Fig. 11(b)). In case of Al_2O_3-water, heat transfer rate decreases faster than Cu-

water as plotted in Figs. 11(a) and 11(b). To analyze the flow behavior result, stream lines are also plotted in Fig. 12.

5. Conclusion

In this paper we have analyzed the effects of each inclined magnetic field, velocity slip and thermal radiation on flow of nanofluid past over a stretching sheet. This study is examined for prescribed surface temperature and two types of nanofluid namely: Cu-water and Al_2O_3-water. Acquired the inclined magnetic field exist enforce with an aligned angle where the aligned angle varies from 0 to $\pi/2$. The following prevailed particular consequences are:

i. Velocity profile of nanofluid decreases with increasing values of nanoparticle volume fraction ϕ, magnetic parameters M_2, γ and slip parameter L for Cu-water/ Al_2O_3-water.

ii. Velocity profile behavior is opposite for each Cu-water and Al_2O_3-Water by gaining the rates of nanoparticles volume fraction ϕ .

iii. Temperature profile increases for each value of nanoparticles volume fraction ϕ, magnetic parameter, adjusted angle γ and velocity slip parameter in case of both Cu −water and Al_2O_3 −water.

iv. The local skin friction coefficient gains with enhancing in the values of magnetic parameter and aligned angle of magnetic field in situation respecting both Cu −water and Al_2O_3 −water. Moreover, it is observed that the local skin friction coefficient does not affected by magnetic parameter at $\gamma = 0°$ and Cu-water nanofluid but it is enhancing rapidly as compared to Al_2O_3-water.

v. Local Nusselt number increases with the value of magnetic parameter for both Cu-Water and Al_2O_3-Water. The heat transfer rate is higher for Al_2O_3-Water as compared to the Cu-Water. Local Nusselt number reduces along with estimations of radiation parameter, velocity slip parameter and aligned angle of magnetic field.

Acknowledgment

Authors would like to acknowledge and express their gratitude to the United Arab Emirates University, Al Ain, UAE for providing the financial support with Grant No. 31S212-UPAR (9) 2015.

References

[1] K. Abdul Hakeem , P. Renuka, N. Vishnu Ganesh, R. Kalaivanan, B. Ganga, Influence of inclined Lorentz forces on boundary layer flow of Casson fluid over an impermeable stretching sheet with heat transfer, Journal of Magnetism and Magnetic Materials 401 (2016) 354–361.

[2] O.D. Makinde, W. A. Khan, Z. H. Khan, Buoyancy effects on MHD stagnation point flow and heat transfer of a nanofluid past a convectively heated stretching/shrinking sheet, International Journal of Heat Mass Transfer. 62 (2013) 526–533.

[3] M. M. Rahman, I. A. Eltaye, Radiative heat transfer in a hydromagnetic nanofluid past a non-linear stretching surface with convective boundary condition, Meccanica, 48 (2013) 601–615.

[4] N. S. Akbar, S. Nadeem, Rizwan Ul Haq, Shiwei Ye, MHD stagnation point flow of Carreau fluid toward a permeable shrinking sheet: Dual solutions, Ain Shams Engineering Journal 5(4) (2014) 1233-1239.

[5] M.M. Rashidi, N. Vishnu Ganesh, A.K. Abdul Hakeem, B. Ganga, Buoyancy effect on MHD flow of nanofluid over a stretching sheet in the presence of thermal radiation, Journal of Molecular Liquids 198 (2014) 234-238.

[6] A Mastroberardino, Antonio, and J. I. Siddique. Magnetohydrodynamic Stagnation Flow and Heat Transfer toward a Stretching Permeable Cylinder, Advances in Mechanical Engineering 6 (2014) 419568.

[7] Akbar, Noreen Sher, Abdelhalim Ebaid, and Z. H. Khan. Numerical analysis of magnetic field effects on Eyring-Powell fluid flow towards a stretching sheet. Journal of Magnetism and Magnetic Materials 382 (2015) 355-358.

[8] M. Sheikholeslami, D.D.Ganji, M.YounusJaved, R.Ellahi, Effect of thermal radiation on magnetohydrodynamics nanofluid flow and heat transfer by means of two phase model, Journal of Magnetism and Magnetic Materials 374 (2015) 36-43.

[9] M. Turkyilmazoglu, M. Analytic heat and mass transfer of the mixed hydrodynamic/thermal slip MHD viscous flow over a stretching sheet. International Journal of Mechanical Sciences 53.10 (2011) 886-896.

[10] M. Sheikholeslami, R. Ellahi, Three dimensional mesoscopic simulation of magnetic field effect on natural convection of nanofluid, International Journal of Heat and Mass Transfer, 89 (2015) 799–808,

[11] R. Ellahi, M. Hassan, A. Zeeshan, Shape effects of nanosize particles in Cu-H_2O nanofluid on entropy generation, International Journal of Heat and Mass Transfer, 81 (2015) 449–456.

[12] M. Akbarzadeh, S. Rashidi, M. Bovand, R. Ellahi, A sensitivity analysis on thermal and pumping power for the flow of nanofluid inside a wavy channel, Vol. 220, (2016), 1-13, Journal of Molecular Liquids.

[13] A. Zeeshan, A. Majeed, R. Ellahi, Effect of magnetic dipole on viscous ferro-fluid past a stretching surface with thermal radiation, Journal of Molecular Liquids, Vol. 215 (2016) 549-554.

[14] S.U. Rahman, R. Ellahi, S. Nadeem, Q.M. Zaigham Zia, Simultaneous effects of nanoparticles and slip on Jeffrey fluid through tapered artery with mild stenosis, Journal of Molecular Liquids, 218 (2016) 484-493.

[15] Mohsen Sheikholeslami, Davood Domiri Ganji, M. Younus Javed, R. Ellahi, Effect of thermal radiation on nanofluid flow and heat transfer using two phase model, Journal of Magnetism and Magnetic Materials, 374 (2015) 36-43.

[16] Maxwell, J. C., A Treatise on Electricity and Magnetism, 2nd ed., vol. 1, Clarendon Press, Oxford, U.K., (1881).

[17] Choi SUS, Enhancing thermal conductivity of fluids with nanoparticles. In: Int. Mech. Eng Cong and Exp, ASME FED 231/MD. 66 (1995) 99-105.

[18] X.-Q. Wang and A. S. Mujumdar, “Heat transfer characteristics of nanofluids: a review,” International Journal of Thermal Sciences, 46(1) (2007), 1–19.

[19] S. K. Das, Sarit Kumar, Stephen US Choi, and Hrishikesh E. Patel. "Heat transfer in nanofluids—a review." Heat transfer engineering 27. 10 (2006), 3-19.

[20] L. Cheng, F. E. P. Bandarra, and J. R. Thome, “Nanofluid two-phase flow and thermal physics: a new research frontier of nanotechnology and its challenges,” Journal of Nano science and Nanotechnology, 8(7) (2008) 3315–3332.

[21] Eastman, J. A., et al. "Enhanced thermal conductivity through the development of nanofluids." MRS proceedings. Vol. 457. Cambridge University Press, 1996.

[22] Rizwan Ul Haq, N.F.M. Noor, Z.H. Khan, Numerical Simulation of Water base Magnetite nanoparticles between Two Parallel Disks, Advanced Powder Technology, 27(4) (2016) 1568-1575.

[23] Rizwan Ul Haq, S.T. Hussain, Z.H. Khan, Z. Hammouch, Flow and Heat transfer analysis of Water and Ethylene Glycol based *Cu* nanoparticles between two parallel disks with Suction/Injection effects, Journal of Molecular Liquids, 221 (2016) 298–304.

[24] H. Masuda, A. Ebata, K. Teramae, N. Hishinuma, Alteration of thermal conductivity and viscosity of liquid by dispersing ultra-fine particles, Netsu Bus-sei (Japan), 7 (1993) 227e233.

[25] J. Buongiorno, Convective transport in nanofluids, ASME Journal of Heat Transfer,(128) (2006), 240–250.

[26] S Ahmad, A M Rohni and I Pop, Blasius and Sakiadis problems in nanofluids, Acta Mechanica, 218 (2011) 195-204.

[27] R. K. Tiwari and M. K. Das, Heat Transfer Augmentation in a Two-Sided Lid-Driven Differentially Heated Square Cavity Utilizing Nanofluids, International Journal of Heat and Mass Transfer, 50 (2007) 2002-2018.

[28] A. K. Abdul Hakeem, R. Kalaivanan, N. Vishnu Ganesh, B. Ganga, Effect of partial slip on hydromagnetic flow over a porous stretching sheet with non-uniform heat source/sink, thermal radiation and wall mass transfer, Ain Shams Engineering Journal. 5 (2014) 913–922.

[29] Hakan F. Oztop, Eiyad Abu-Nada, Numerical study of natural convection in partially heated rectangular enclosures filled with nanofluids, International Journal of Heat and Fluid Flow, 29(5) (2008) 1326-1336

[30] Study of stream wise transverse magnetic fluid flow with heat transfer around a porous obstacle, Journal of Magnetism and Magnetic Materials, 378 (2015) 128–137.

[31] Study on magnetohydrodynamic nanofluid by means of single and multi-walled carbon nanotubes suspended in a salt water solution, IEEE Transactions on Nanotechnology, 14 (4) (2015) 726 – 734.

[32] Simulation of ferrofluid flow for magnetic drug targeting using Lattice Boltzmann method, Journal of Zeitschrift Fur Naturforschung A, Verlag der Zeitschrift für Naturforschung. 70 (2) (2015) 115–124.

[33] Influence of induced magnetic field and heat flux with the suspension of carbon nanotubes for the peristaltic flow in a permeable channel, Magnetism and Magnetic Materials, Vol. 381, (2015) 405–415.

[34] Electrohydrodynamic nanofluid hydrothermal treatment in an enclosure with sinusoidal upper wall, Applied Sciences, 5 (2015) 294-306.

[35] Sohail Nadeem, Rizwan Ul Haq, Zafar Hayat Khan, Heat transfer analysis of water-based nanofluid over an exponentially stretching sheet, Alexandria Engineering Journal, 53(1) (2014) 219-224.

[36] Rizwan Ul Haq, Zafar Hayat Khan, Waqar Ahmed Khan, Thermophysical effects of carbon nanotubes on MHD flow over a stretching surface, Physica E: Low-dimensional Systems and Nanostructures, 63 (2014) 215-222.

[37] S. Saleem, S. Nadeem, Rizwan Ul Haq, Buoyancy and metallic particle effects on an unsteady water-based fluid flow along a vertically rotating cone, The European Physical Journal Plus, 129 (2014) 213.

[38] Rizwan Ul Haq, Sohail Nadeem, Z.H. Khan, N.F.M. Noor, Convective heat transfer in MHD slip flow over a stretching surface in the presence of carbon nanotubes, Physica B: Condensed Matter, 457(15) (2015) 40-47.

[39] Rizwan Ul Haq, D. Rajotia, N. F. M. Noor, Thermophysical Effects of Water Driven Copper Nanoparticles on MHD Axisymmetric Permeable Shrinking Sheet: Dual Nature Study, The European Physical Journal E, 39 (2016) 33.

[40] S. T. Hussain, Rizwan Ul Haq, Z. H. Khan, S. Nadeem, Water Driven Flow of Carbon nanofluid nanotubes in a rotating channel, Journal of Molecular Liquid, 214, (2016) 136–144.

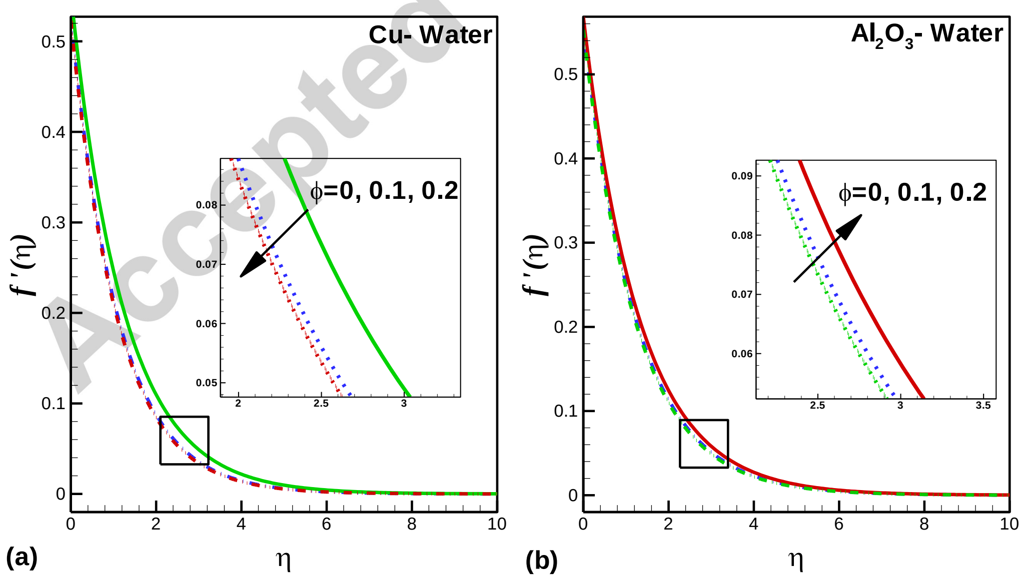

Fig.1: Variation of velocity profile $f'(\eta)$ for different values of ϕ with $\beta = 1, M_2 = 0.2$ and $\gamma = \pi/4$ (a) Cu −water (b) Al_2O_3 −water.

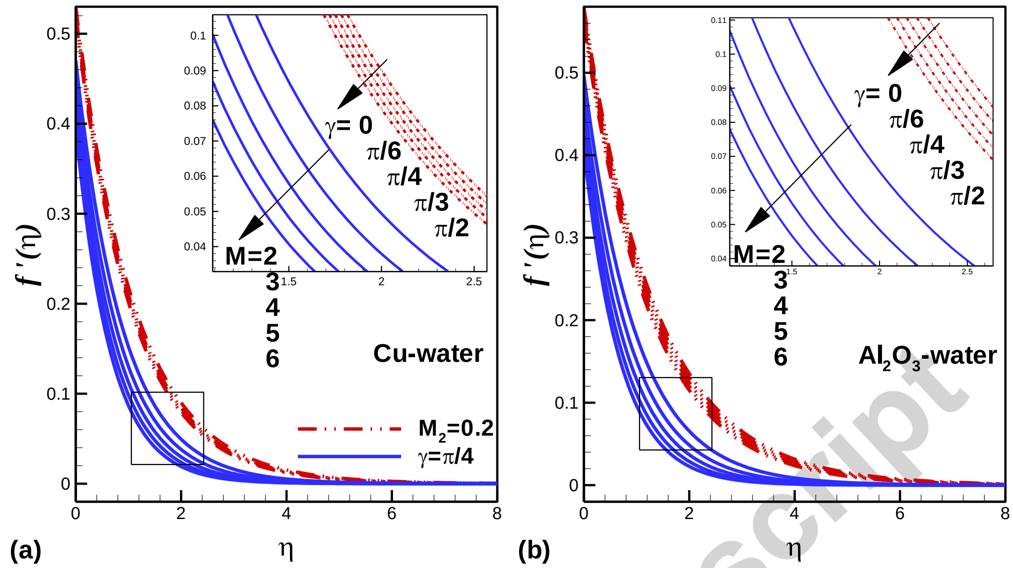

Fig.2: Variation of velocity profile $f'(\eta)$ for different values of M_2 and γ with $\beta = 1, \phi = 0.2$ (a) Cu −water (b) Al_2O_3 −water.

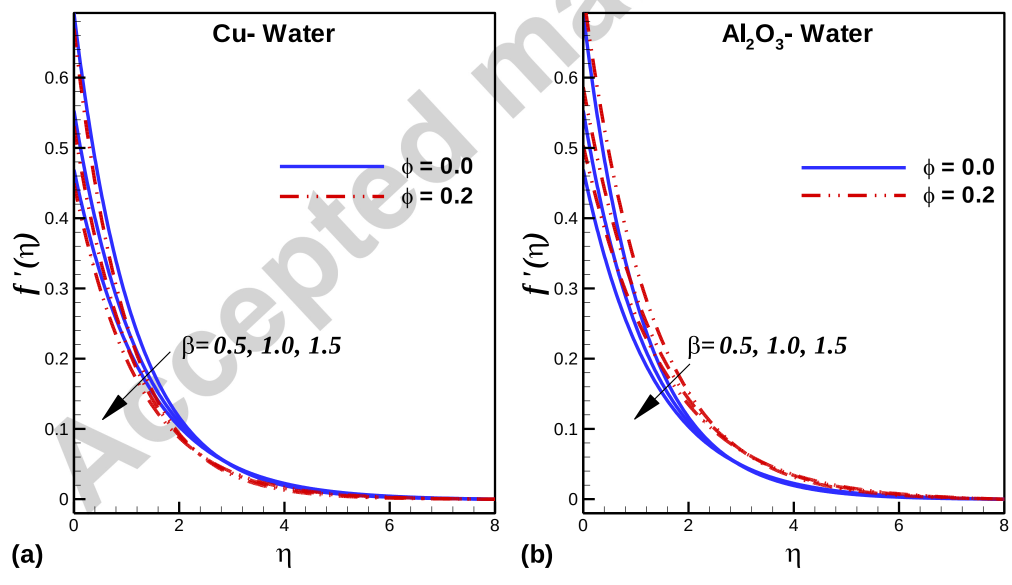

0

Fig.3: Variation of velocity profile $f'(\eta)$ for different values of β and ϕ when $M_2 = 0.2, \gamma = \pi/4$ (a) Cu −water (b) Al_2O_3 −water.

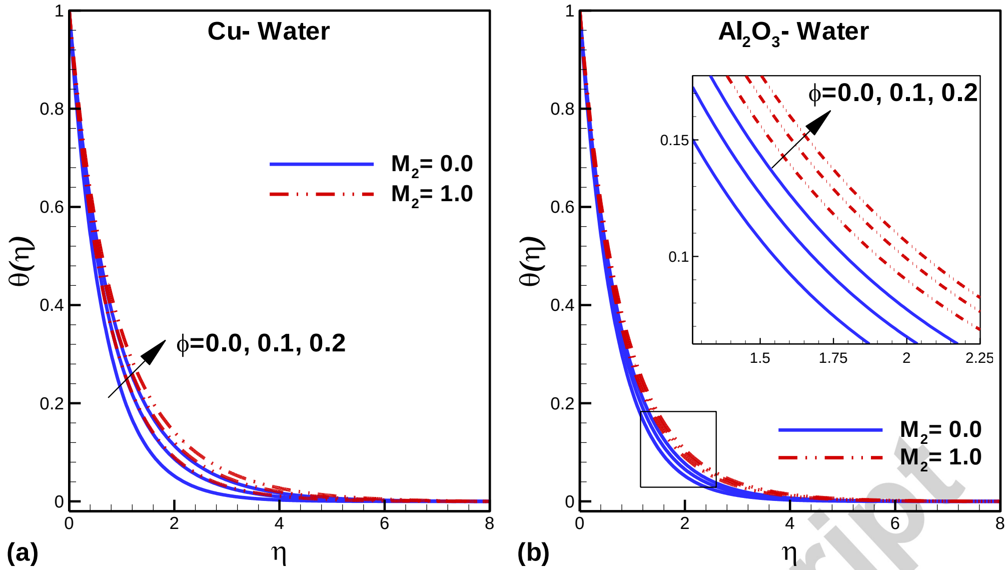

Fig.4: Variation of temperature profile $\theta(\eta)$ for different values of M_2 and ϕ with $\beta = 0.5, N = 0.5,\ \gamma = \pi/4$ (a) Cu −water (b) Al_2O_3 −water.

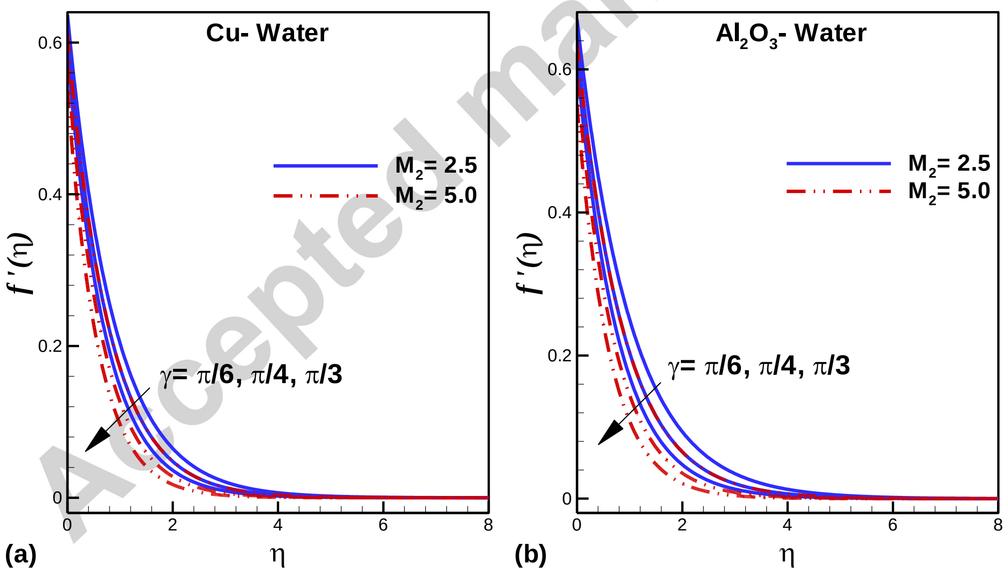

Fig.5: Variation of temperature profile $\theta(\eta)$ for different values of γ and M_2 with $\beta = 0.5, N = 0.5,\ \gamma = \pi/4$ (a) Cu −water (b) Al_2O_3 −water.

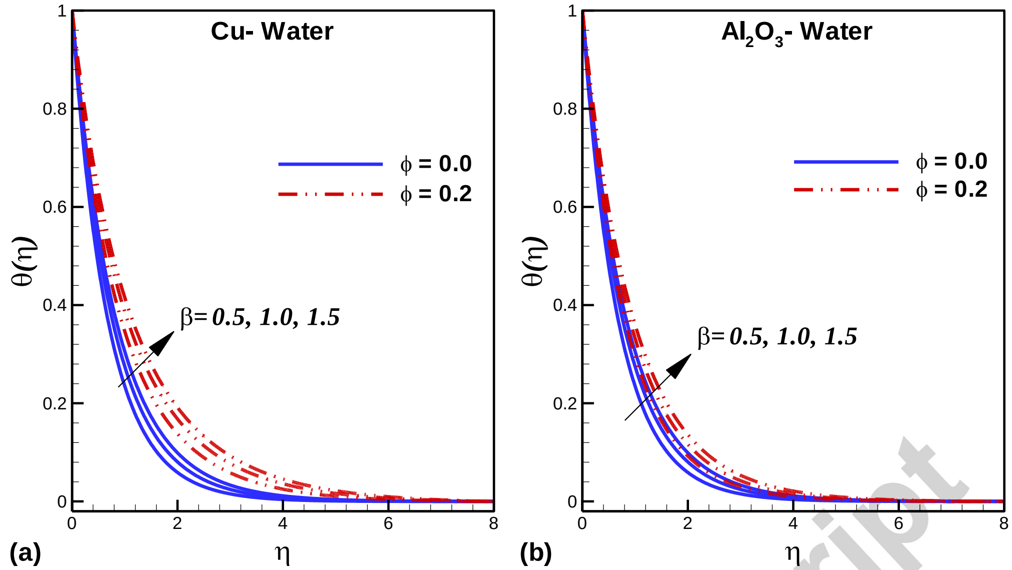

Fig.6: Variation of temperature profile $\theta(\eta)$ for different values of L and ϕ with $M_2 = 0.2, N = 0.5,\ \gamma = \pi/4$ (a) Cu −water (b) Al_2O_3 −water.

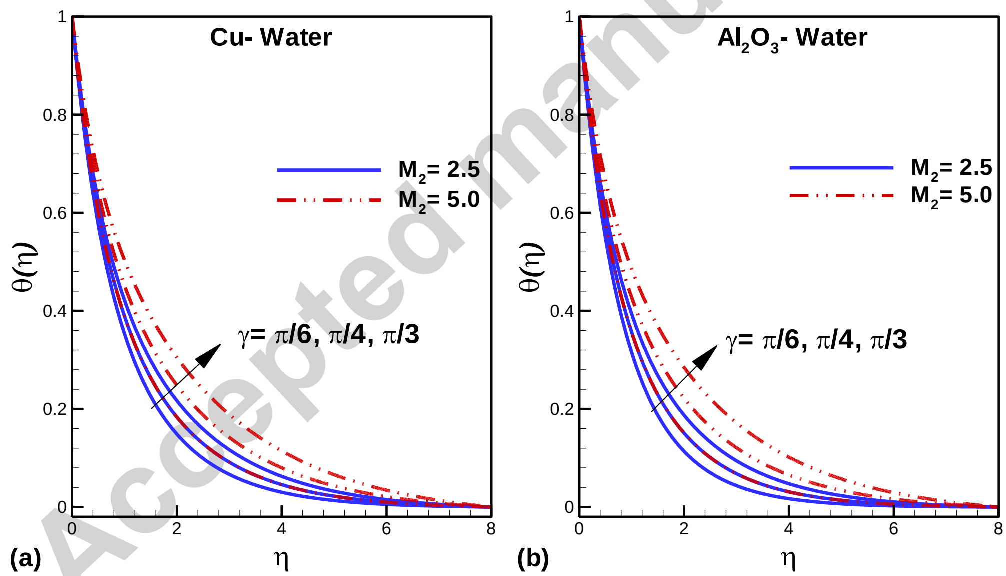

Fig.7: Variation of temperature profile $\theta(\eta)$ for different values of γ and M_2 with $\beta = 0.5, N = 0.5$(a) Cu-Water (b) Al_2O_3-Water.

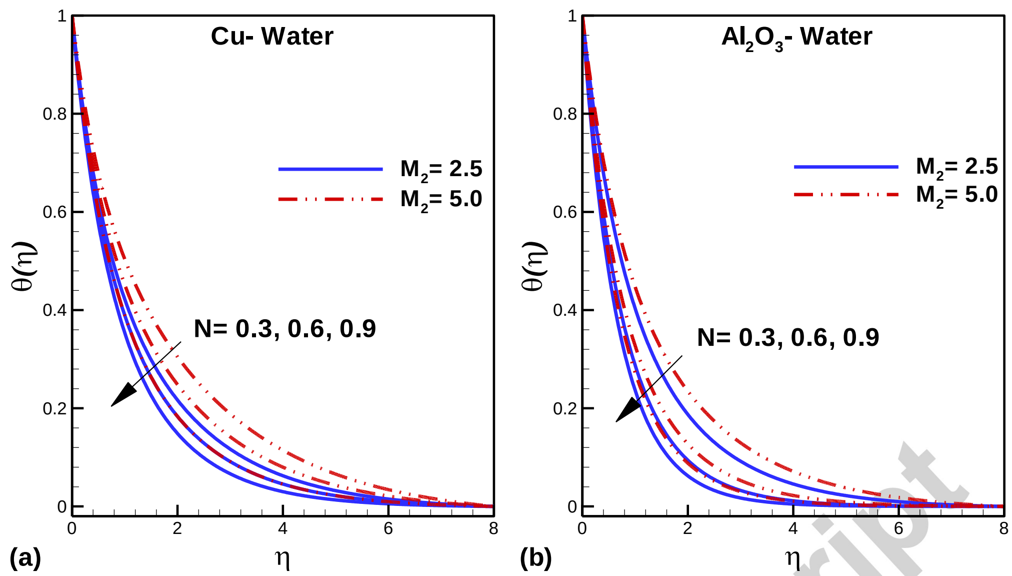

Fig.8: Variation of temperature profile $\theta(\eta)$ for different values of N and M_2 with $\beta = 0.5, N = 0.5$, (a) Cu −water (b) Al_2O_3 −water.

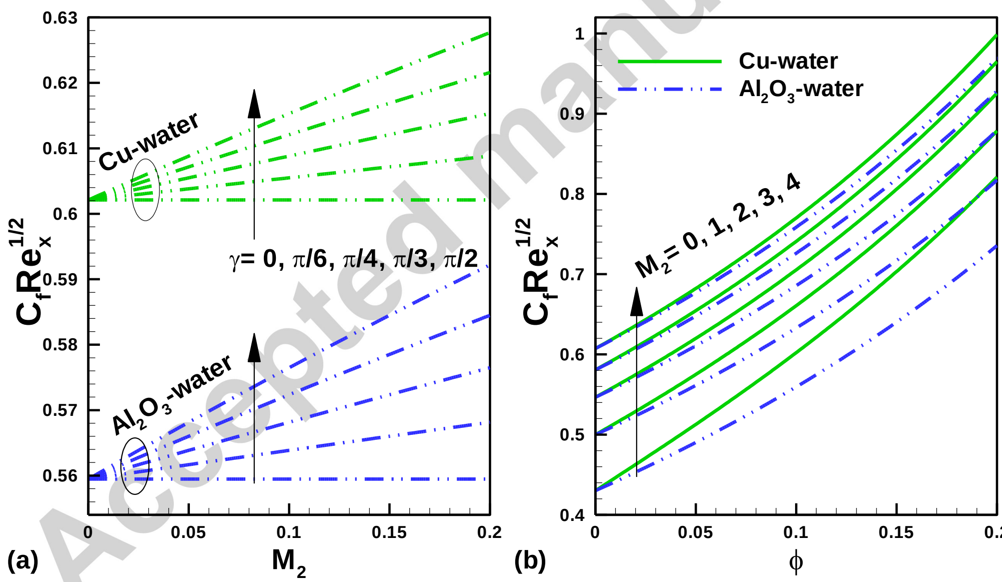

Fig.9: Variation of skin friction for (a) M_2 and γ when $\phi = 0.2$, $\beta = 1$ (b) M_2 and ϕ when $\gamma = 45°$, $\beta = 1$.

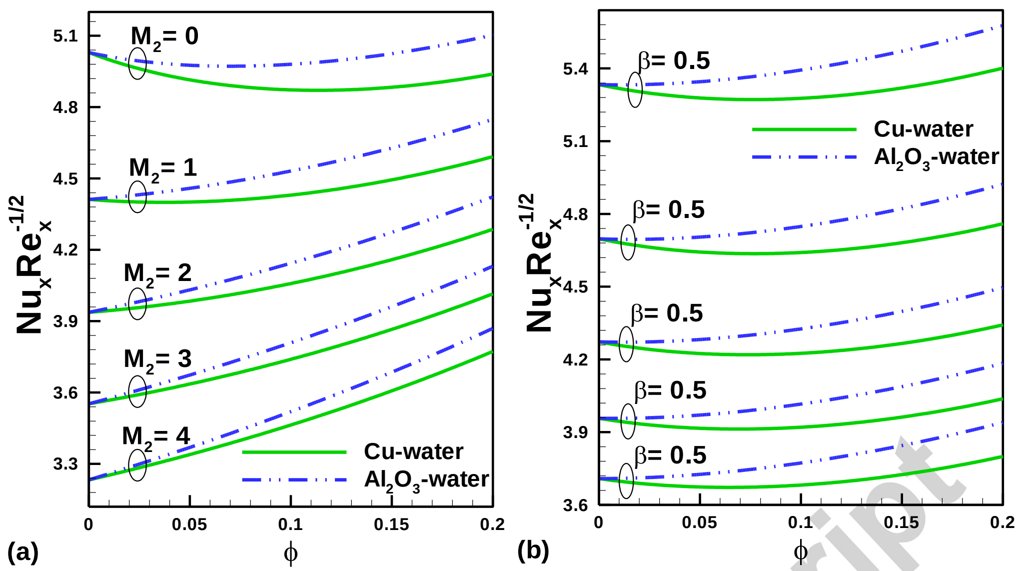

Fig.10: Variation of local Nusselt number for (a) M_2 and ϕ when $\gamma = 45°$, $\beta = 1$, $N = 0.5$ (b) β and ϕ when $\gamma = 45°, M_2 = N = 0.5$.

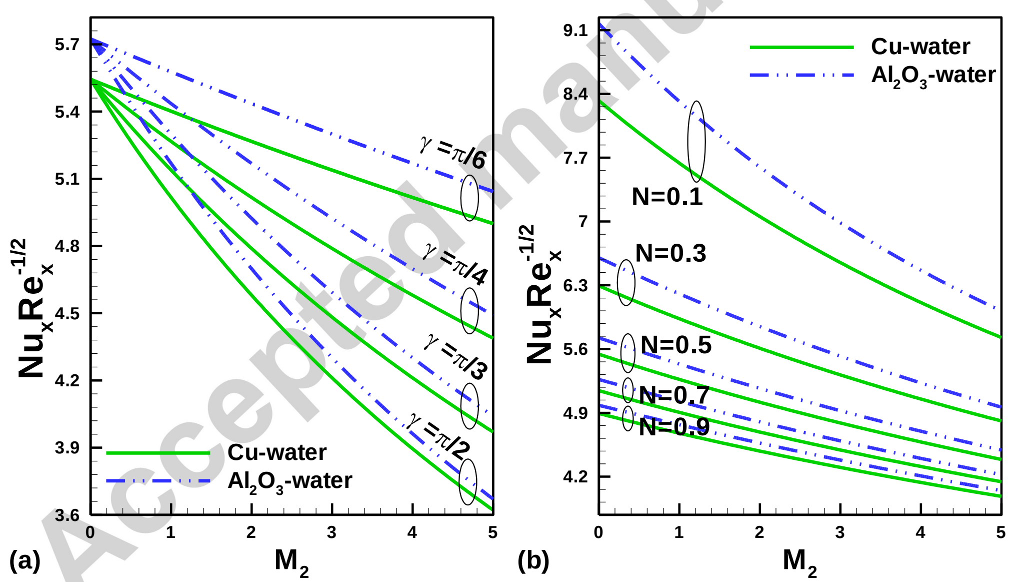

Fig.11: Variation of local Nusselt number for (a) M_2 and γ when $\phi = 0.2, \beta = N = 0.5$ (b) M_2 and N when $\gamma = 45°, \phi = 0.2, \beta = 0.5$.

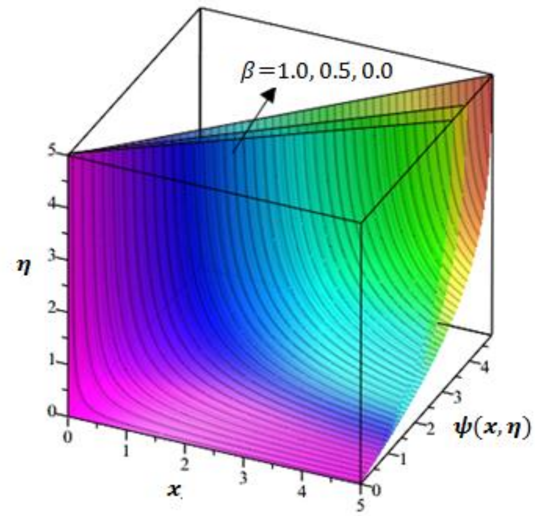

Fig.12: Stream lines behavior for various values of slip parameter.

Highlights

- Nanofluid fluid flow with inclined Lorentz forces is purposed.
- Cu-water and Al_2O_3-water are reported over a stretched flow.
- Hartmann number resists the flow motion of each mixture at the surface.
- Slip parameter decrease the velocity and increase the temperature profile.
- Cu-water attained higher skin friction as compare to the Al_2O_3-water.